JOURNAL OF AGRICULTURAL AND FOOD CHEMISTRY

pubs.acs.org/JAFC Article

Hierarchical Reactivity of Enzyme-Mediated Phosphorus Recycling from Organic Mixtures by *Aspergillus niger* Phytase

Mina Solhtalab, Annaleise R. Klein, and Ludmilla Aristilde*

Cite This: *J. Agric. Food Chem.* 2021, 69, 2295−2305 Read Online

ACCESS | Metrics & More | Article Recommendations | Supporting Information

ABSTRACT: Biological recycling of inorganic phosphorus (P_i) from organic phosphorus (P_o) compounds by phosphatase-type enzymes, including phytases, is an important contributor to the pool of bioavailable P to plants and microorganisms. However, studies of mixed-substrate reactions with these enzymes are lacking. Here, we explore the reactivity of a phytase extract from the fungus *Aspergillus niger* toward a heterogeneous mixture containing, in addition to phytate, different structures of environmentally relevant P_o compounds such as ribonucleotides and sugar phosphates. Using a high-resolution liquid chromatography−mass spectrometry method to monitor simultaneously the parent P_o compounds and their by-products, we captured sequential substrate-specific evolution of P_i from the mixture, with faster hydrolysis of multiphosphorylated compounds (phytate, diphosphorylated sugars, and di- and tri-phosphorylated ribonucleotides) than hydrolysis of monophosphorylated compounds (monophosphorylated sugars and monophosphorylated ribonucleotides). The interaction mechanisms and energies revealed by molecular docking simulations of each P_o compound within the enzyme's active site explained the substrate hierarchy observed experimentally. Specifically, the favorable orientation for binding of the negatively charged phosphate moieties with respect to the positive potential surface of the active site was important. Collectively, our findings provide mechanistic insights about the broad but hierarchical role of phytase-type enzymes in P_i recycling from the heterogeneous assembly of P_o compounds in agricultural soils or wastes.

KEYWORDS: *phytase, organic phosphorus, substrate mixtures, liquid chromatography−mass spectrometry, molecular docking simulations, Aspergillus niger*

INTRODUCTION

Phosphorus (P), which is a key nutrient for all organisms, is essential in the form of orthophosphate (P_i) for optimal plant growth,[1] agricultural productivity,[2] and important soil microbial processes.[3] Organic P (P_o) compounds represent 30−65% of soil P,[4,5] which include inositol phosphates, sugar phosphates, ribonucleotides, and nucleic acids.[6,7] Because these P_o compounds are not directly available for biological assimilation,[5] plants and microorganisms employ a suite of phosphatase-type enzymes to extract P_i hydrolytically from plant residues and soil organic matter.[8,9] Of particular interest to the P turnover in P_i-deficient agricultural soils are the phytases,[10,11] a subset of phosphatase enzymes that specifically targets the stepwise dephosphorylation of myo-inositol hexakisphosphate (myo-IP_6 or phytate) (Figure 1A),[12] the main P storage compound in plants, seeds, and grains.[13] In fact, the abundance of a phytase gene was found to be 4-fold higher in soils deficient in P_i relative to soils enriched in P_i,[11] thus implicating the role of phytase in relieving P_i deficiency in soils.[10] Furthermore, the addition of phytases in the animal feed has been instrumental in enhancing P nutrient availability.[14] In addition to myo-IP_6 and its related by-products, phytases have been shown to catalyze the dephosphorylation of other P_o compounds such as sugar phosphates and ribonucleotides.[15] However, the activity of phytase enzymes on organic mixtures has not yet been investigated. In this study, we explore the reactivity of phytase A (PhyA) from the fungus *Aspergillus niger*,[16] a predominant species in the plant rhizosphere[17] toward recycling P_i from a heterogenous mixture of environmentally relevant P_o compounds.

Previous studies have been conducted for PhyA only in single-substrate scenarios with myo-IP_6, a sugar phosphate (glucose-6-phosphate, G6P), or a ribonucleotide (adenosine monophosphate, AMP; adenosine diphosphate, ADP; or adenosine triphosphate, ATP).[18−21] The dephosphorylation rate for one specific compound in these single-substrate experiments does not account for the competition for accessing the PhyA active site by a different substrate.[6,7,22] Because of the heterogeneity of substrates in environmentally relevant mixtures, a competition between different P_o substrates is expected to result in different rates of hydrolysis, compared to the single-substrate scenario.[23,24] This mixture effect, which underlies inconsistencies between in vitro kinetic parameters and in vivo data, has received much attention in enzyme assays in molecular biochemistry and drug discovery studies.[25,26] Alternative to single-substrate experiments, "internal competition" experiments with multiple substrates in the reaction mixture aimed at monitoring the preference of an enzyme for a

Received: September 15, 2020
Revised: November 10, 2020
Accepted: November 24, 2020
Published: December 11, 2020

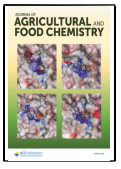

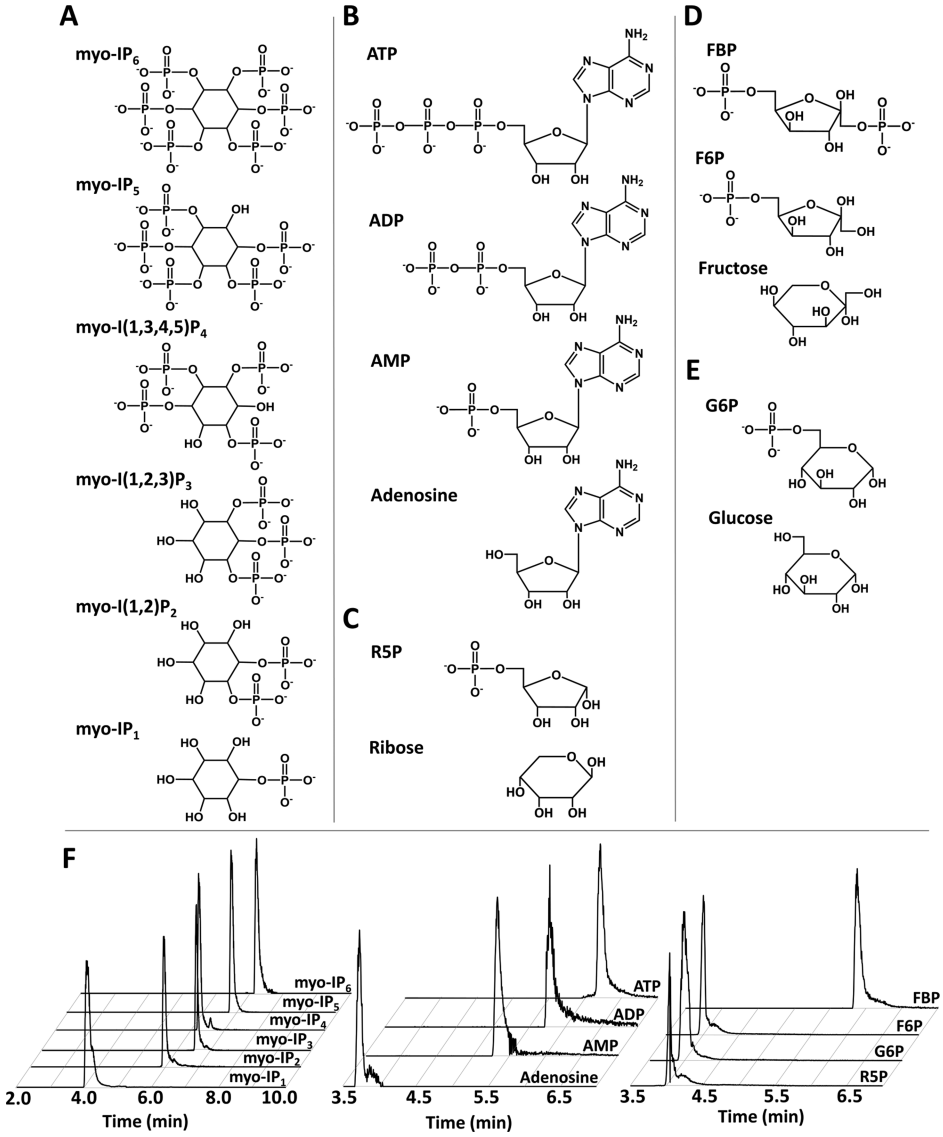

Figure 1. Chemical structures and extracted ion chromatograms of investigated P_o compounds. In A, from top to bottom, myo-IP_6, myo-IP_5, myo-IP_4, myo-IP_3, myo-IP_2, myo-IP_1; shown for myo-IP_4, myo-IP_3 and myo-IP_2 are the reported structures for the most abundant isomers in the hydrolysis products of PhyA.[49,50] In B, ATP, ADP, AMP, and adenosine. In C, ribose 5-phosphate (R5P) and D-ribose. In D, fructose-1,6-biphosphate (FBP), fructose-6-phosphate (F6P), and fructose. In E, glucose 6-phosphate (G6P) and glucose. In F, extracted ion chromatograms: myo-IP_6 (658.8541), myo-IP_5 (578.8878), myo-IP_4 (498.9214), myo-IP_3 (418.9551), myo-IP_2 (338.9888), myo-IP_1 (259.0224), FBP (338.9888), F6P (259.0224), G6P (259.0224), R5P (229.0119), ATP (505.9885), ADP (426.0221), AMP (346.0558) and adenosine (266.0895). The EICs were obtained at the specified m/z channel with a 25 ppm mass tolerance. The LC−MS response intensity was different for the compounds at equivalent concentrations (10 μM).

specific substrate in the mixture.[24,27] This approach, in which the reaction rates are calculated by simultaneously monitoring the concentrations of multiple substrates or multiple products,[24,25] has been employed in enzyme assay studies of complex biological mixtures[26] but has received little attention within the context of enzyme reactivity with environmentally relevant substrate mixtures.

Here, we combine high-resolution liquid chromatography−mass spectrometry (LC−MS) with molecular modeling and implicate the internal competition approach to investigate the reactivity of PhyA toward a mixture of P_o compounds, containing myo-IP_6 (the endogenous substrate of the enzyme), one ribonucleotide (ATP), two sugar phosphates [G6P and ribose-5-phosphate (R5P)], and an intermediate in cellular carbon metabolism (fructose-1-6-bisphosphate, FBP) (Figure 1A). Monitoring only the P_i concentration, which is typically determined by the phosphomolybdate spectrophotometric method,[28] does not capture substrate-specific P_i in mixed-substrate reactions. Therefore, we developed a LC−MS method to monitor simultaneously the disappearance of each P_o substrate and the evolution of their sequential dephosphorylated organic by-products (Figure 1). Using the LC−MS data, we quantified the contribution of each specific P_o compound in the mixture to the total recycled P_i. Importantly, we were able to compare the reaction rates of the parent and by-product compounds in the mixed-substrate scenarios to those obtained for the corresponding compounds in single-substrate scenarios. With respect to the mechanisms of phytase reactivity, prior studies have focused on the catalytic mechanisms of phytases with its endogenous substrate (i.e.,

https://dx.doi.org/10.1021/acs.jafc.0c05924
J. Agric. Food Chem. 2021, 69, 2295−2305

phytate).[29,30] No atomic-scale mechanistic study has been conducted on the substrate binding selectivity of PhyA for different P_o compounds. Here, we performed molecular docking simulations of the enzyme−substrate complexes for each investigated P_o compound to shed light on the mechanistic reasonings of the experimentally determined substrate selectivity based on the simulated interaction mechanisms and energies.[31] Of agricultural importance, our experimental and computational findings provide new insights into the role of phytases and related phosphatases widely secreted by both plants and microorganisms in mediating P_i recycling from organic assemblages in environmental matrices.

MATERIALS AND METHODS

Materials. Details on the purchase of chemical compounds and the enzyme are provided in Appendix A in the Supporting Information.

Dephosphorylation Reactions of P_o Compounds Catalyzed by *A. niger* Phytase Extract. For single-substrate reactions, we reacted the phytase extract (50 μL from the purchased batch; 3 U/mL) with myo-IP_6 (400 μM), each of the ribonucleotides (ATP, ADP, or AMP at 400 μM), or each of the sugar-phosphates (FBP, F6P, G6P, or R5P at 400 μM). The substrate solution (50 mL) was prepared with sodium acetate buffer (0.1 M, pH 5.3) in a 125-mL Erlenmeyer flask and equilibrated for 30 min at 37 °C. After addition of the PhyA extract to the substrate solution, the solution was well-mixed and then left to incubate at 37 °C at moderate shaking (110 rpm) before time-course measurements. At a specific time point (0.5 min, 5 min, 10 min, 20 min, 1 h, 2 h, 6 h, 12 h, 24 h, or 48 h), 1 mL HCl (1 M) was added to a 1 mL aliquot of the reaction mixture to stop the reaction and immediately immersed in ice. Control experiments were conducted with each substrate without the PhyA extract. For the mixed-substrate reactions, the PhyA extract was reacted with a solution mixture containing myo-IP_6, ATP, FBP, G6P, and R5P (400 μM each); therefore, ADP, AMP, and F6P were the reaction products in the mixture. To evaluate the influence of myo-IP_6 on the PhyA activity toward other substrates, we also reacted the PhyA extract with the same solution mixture in the absence of myo-IP_6. Control experiments were conducted with the mixtures without the phytase extract. All experiments were run in three or more independent replicates. All samples were kept at 4 °C until analysis.

Analysis of P_o Substrates and Reaction Products by LC−MS. In preparation for LC−MS analysis, the acidified samples obtained above were neutralized with NaOH and diluted with Milli-Q water to be within the concentration range of the substrate calibration curve (0.5−20 μM). Similarly, the samples frozen in liquid nitrogen (discussed later) were also diluted with Milli-Q water prior to the LC−MS run. The kinetic samples were analyzed via reverse-phase ultrahigh-performance LC (ThermoFisher Scientific Dionex UltiMate 3000, Waltham, MA, USA) coupled to high-resolution/accurate-mass spectrometry (ThermoFisher Scientific Q Exactive Quadrupole-Orbitrap hybrid MS) with electrospray ionization run in a full scan negative mode. Building on our in-house metabolomics method,[32] we developed an optimized LC−MS method to detect ATP, ADP, AMP, adenosine, FBP, F6P, G6P, R5P, myo-IP_6, and their lower phosphorylated by-products, that is, myo-inositol pentakisphosphate (myo-IP_5), myo-inositol tetrakisphosphate (myo-IP_4), myo-inositol triphosphate (myo-IP_3), myo-inositol biphosphate (myo-IP_2), and myo-inositol monophosphate (myo-IP_1), simultaneously (Figure 1). Details of the chromatographic separation procedure are provided in Appendix B (Supporting Information). To measure the sugar by-products (fructose, glucose, and ribose) in the experiments with sugar phosphates (FBP, F6P, G6P, or R5P), we employed a recently published LC−MS method[33] for simultaneous carbohydrate quantitation. Direct measurements of P_i concentration in samples were obtained using the molybdenum-blue assay,[28] which are detailed in Appendix B (Supporting Information).

Analytical Models of Enzymatic Dephosphorylation Reactions. Using nonlinear regression modeling (SigmaPlot 14.0) of the LC−MS data of P_o compounds and their organic dephosphorylated by-products, we determined the enzymatic transformation rate constants (k_X, where X represents the compound name) for different parent P_o compounds (ATP, FBP, G6P, and R5P) and their by-products (ADP, AMP, and F6P) in both single-substrate and mixed-substrate reactions. Because of the very fast catalysis of myo-IP_6 dephosphorylation, we were not able to develop analytical models of the myo-IP_6 reaction with the enzyme. The governing differential equations and the corresponding analytical solutions used for modeling the kinetics variations of all species-concentrations are detailed in Appendix C (Supporting Information). Here, we only show the corresponding analytical solutions used to determine the dephosphorylation rates of the P_o compounds.

In mixed-substrate reactions, considering the sequential dephosphorylation of ATP and its by-products ADP and AMP, eqs 1−3 were used, respectively.

$$[\mathrm{ATP}] = [\mathrm{ATP}]_0 \exp(-k_{\mathrm{ATP}} t) \tag{1}$$

$$[\mathrm{ADP}] = \frac{k_{\mathrm{ATP}}[\mathrm{ATP}]_0}{k_{\mathrm{ADP}} - k_{\mathrm{ATP}}} \exp(-k_{\mathrm{ATP}} t) + \left([\mathrm{ADP}]_0 - \frac{k_{\mathrm{ATP}}[\mathrm{ATP}]_0}{k_{\mathrm{ADP}} - k_{\mathrm{ATP}}}\right) \exp(-k_{\mathrm{ADP}} t) \tag{2}$$

$$[\mathrm{AMP}] = \frac{k_{\mathrm{ADP}} k_{\mathrm{ATP}}[\mathrm{ATP}]_0}{(k_{\mathrm{ADP}} - k_{\mathrm{ATP}})(k_{\mathrm{AMP}} - k_{\mathrm{ATP}})} \exp(-k_{\mathrm{ATP}} t) + \frac{k_{\mathrm{ADP}}[\mathrm{ADP}]_0 (k_{\mathrm{ADP}} - k_{\mathrm{ATP}}) - k_{\mathrm{ADP}} k_{\mathrm{ATP}}[\mathrm{ATP}]_0}{(k_{\mathrm{ADP}} - k_{\mathrm{ATP}})(k_{\mathrm{AMP}} - k_{\mathrm{ADP}})} \exp(-k_{\mathrm{ADP}} t) + \frac{k_{\mathrm{ADP}}[\mathrm{ADP}]_0 (k_{\mathrm{AMP}} - k_{\mathrm{ATP}}) - k_{\mathrm{ADP}} k_{\mathrm{ATP}}[\mathrm{ATP}]_0}{(k_{\mathrm{AMP}} - k_{\mathrm{ATP}})(k_{\mathrm{AMP}} - k_{\mathrm{ADP}})} \exp(-k_{\mathrm{AMP}} t) \tag{3}$$

For the sequential dephosphorylation of FBP and its by-product F6P in the mixed-substrate reactions, we used eqs 4 and 5.

$$[\mathrm{FBP}] = [\mathrm{FBP}]_0 \exp(-k_{\mathrm{FBP}} t) \tag{4}$$

$$[\mathrm{F6P}] = \frac{k_{\mathrm{FBP}}[\mathrm{FBP}]_0}{k_{\mathrm{F6P}} - k_{\mathrm{FBP}}} \exp(-k_{\mathrm{FBP}} t) + \left([\mathrm{F6P}]_0 - \frac{k_{\mathrm{FBP}}[\mathrm{FBP}]_0}{k_{\mathrm{F6P}} - k_{\mathrm{FBP}}}\right) \exp(-k_{\mathrm{F6P}} t) \tag{5}$$

For monophosphorylated compounds (XP = G6P or R5P) in mixed-substrate reaction, we use eq 6.

$$[\mathrm{XP}] = [\mathrm{XP}]_0 \exp(-k_{\mathrm{XP}} t) \tag{6}$$

The dephosphorylation rate of each P_o compound (XP = ATP, FBP, ADP, AMP, F6P, G6P, and R5P) as a single substrate in the solution was modeled using eq 6.

Tracking the Hierarchical Evolution of P_i from Mixtures of P_o Compounds. To quantify the contribution of each P_o compound to the P_i recycled from the mixture, we determined the substrate-specific P_i concentration based on the decreased concentration of the corresponding P_o substrate measured by LC−MS [eq 7].

$$[\mathrm{P_i}]_t = [\mathrm{substrate}]_0 - [\mathrm{substrate}]_t \tag{7}$$

where $[\mathrm{P_i}]_t$ and $[\mathrm{substrate}]_t$ represent the concentration of released P_i and the remaining substrate in solution, respectively, at a specific time of reaction; $[\mathrm{substrate}]_0$ is the initial concentration of the parent compound (i.e., myo-IP_6, ATP, FBP, R5P, and G6P), or the highest concentration of the partially dephosphorylated compounds (i.e., ADP, AMP, and F6P) before their subsequent hydrolysis.

Concentration-Dependent Initial Rates of P_o Hydrolysis in Single-Substrate versus Mixed-Substrate Scenarios. We selected ATP and G6P as representatives of multiphosphorylated and monophosphorylated P_o compounds, respectively, to determine

https://dx.doi.org/10.1021/acs.jafc.0c05924
J. Agric. Food Chem. 2021, 69, 2295−2305

the effect of concentrations on the initial rates of P_o hydrolysis. Solutions containing three different concentrations (0.1, 1, or 10 mM) of ATP were prepared in the presence or absence of a P_o mixture, containing myo-IP_6, FBP, G6P, and R5P (each at 0.4 mM concentration), in sodium acetate buffer at pH 5.3. At the same molar concentrations, G6P solutions (0.1, 1, or 10 mM) were prepared in the presence and absence of a P_o mixture, containing 0.4 mM of each of myo-IP_6, ATP, FBP, and R5P. Enzymatic dephosphorylation reactions were started by adding 2 μL of PhyA extract to 100 mL of the reaction solutions. Reaction vessels were incubated in an incubator-shaker maintained at 37 °C. Aliquots of the reaction solutions were poured into microcentrifuge tubes at specific time points, and the reactions were stopped by immersing them in liquid nitrogen. Triplicate controls were run under the same conditions in the absence of the enzyme. The samples were stored at −20 °C until analysis. The P_i concentration in single-substrate reactions was measured using the molybdenum-blue assay[28] (Supporting Information Appendix B). For mixed-substrate reactions, the P_i concentration generated by the targeted substrate (i.e., ATP or G6P) was determined by monitoring the concentrations of the dephosphorylated by-products of each parent compound measured by LC−MS, using eqs 8 and 9 to calculate the P_i released from ATP and G6P, respectively.

$$[P_i]_t = [ADP]_t + (2 \times [AMP]_t) + (3 \times [adenosine]_t) \quad (8)$$

$$[P_i]_t = [glucose]_t \quad (9)$$

The initial velocities of the PhyA-catalyzed reactions were then calculated from the slope of the best fitted trendline through the P_i concentration values at initial time points from the three replicates. For the ratios of initial rates, standard deviations were estimated based on the Taylor series method[34] (Supporting Information Appendix I). An unpaired *t*-test was applied to determine the statistical significance of the differences in initial rates from the single-substrate versus mixture conditions.

Molecular Docking Simulations of P_o Compounds with PhyA. We employed the Discovery Studio software package,[35] which has been used previously to obtain accurate predictions of intermolecular interactions in enzyme−substrate complexes.[36−38] The PhyA structure (PDB ID: 3KQ4), with 2.2 Å resolution, was prepared at pH 5.3 and subjected to two energy-minimization steps in an implicit water solvent. Substrate structures (myo-IP_6, ATP, ADP, AMP, FBP, F6P, G6P, and R5P), obtained from PubChem, were also subjected to energy minimization and prepared at pH 5.3 in an implicit solvent. Docking of the substrates in the active site of the enzyme was performed using the docking protocol CDOCKER in Discovery Studio.[35] After obtaining the optimized substrate−PhyA complex, the CDOCKER energy parameter, which accounts for the internal ligand strain energy and receptor−ligand interaction energy, was used to compare the relative binding favorability of the different compounds.[39] The ligand-interaction protocol in Discovery Studio was employed to determine different types of hydrogen bonding (H-bonding) and electrostatic interactions between each P_o compound and amino acid residues in the PhyA active site. Strong H-bonds were calculated using a donor−acceptor distance less than 3 Å and a donor−hydrogen−acceptor angle cutoff of 160−180°;[40] weak H-bonds were considered at a donor−acceptor distance of less than 3.4 Å and a donor−hydrogen−acceptor angle cutoff of 90−180°. The electrostatic interactions, which included charge−charge and π−charge interactions, were calculated based on the software default parameters (Supporting Information Appendix J).[35] The one-letter codes used to designate the amino acid residues of the enzyme are the following: aspartate (D), arginine (R), glutamate (E), histidine (H), lysine (K), and tyrosine (Y).

RESULTS

Stepwise Dephosphorylation of a Diverse Range of P_o Compounds in a Mixture. The PhyA extract (with 3 U/mL) was reacted with a mixture of P_o compounds (400 μM each): myo-IP_6, ATP, FBP, G6P, and R5P (Figure 2A). By the first 30 s, complete dephosphorylation of myo-IP_6, the endogenous substrate of PhyA, was obtained (Figure 2A). By 20 min, both ATP and FBP were more than 90% dephosphorylated and, simultaneously, their subsequent by-products (ADP and F6P, respectively) reached their maximum

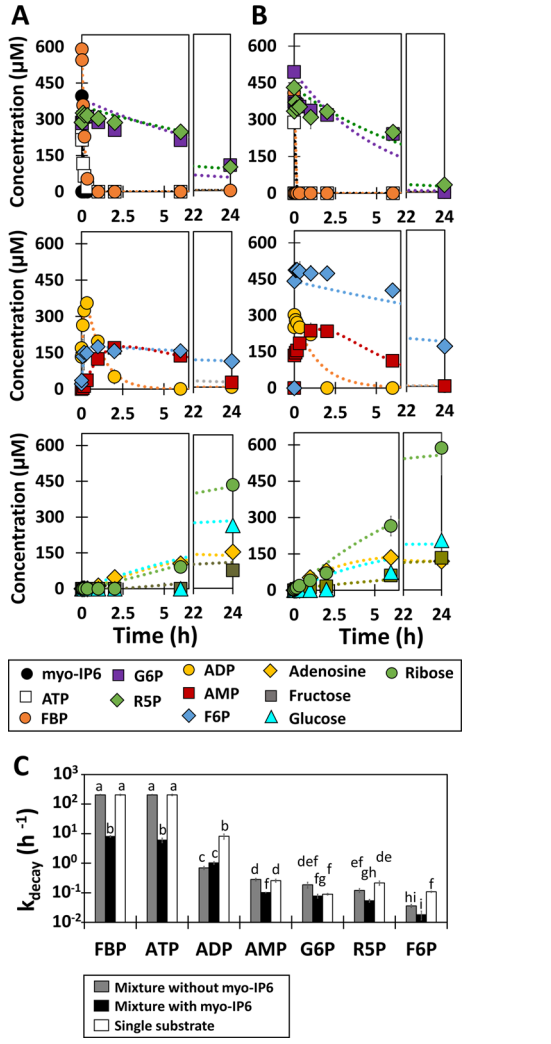

Figure 2. Stepwise dephosphorylation of a mixture of P_o compounds by PhyA extract with (A) or without (B) the natural substrate of the enzyme (myo-IP_6). Upper panels show the dephosphorylation trends of compounds in the starting mixture: ATP (white squares), FBP (orange circles), G6P (purple squares), and R5P (green diamonds), with/without myo-IP_6 (black circles). Middle panels and bottom panels show, respectively, the kinetics of mono-phosphorylated and unphosphorylated daughter products. Dotted lines represent the non-linear regression models (see Materials and Methods). The full kinetic data and the evolution of P_i in solution are shown in Appendix E (Supporting Information). (C) The transformation rate coefficients calculated based on the analytical modeling of kinetic data obtained from a mixed-substrate solution without myo-IP_6 (gray), mixed-substrate solution with myo-IP_6 (black) and single-substrate solution (white). Values that are statistically different (p-value ≤ 0.05) were designated by different letters. The error bars represent the standard error over three replicates. The rate coefficient values for P_o compounds are listed in Table S2 (Supporting Information Appendix F). The progress curves for mixed-substrate solutions are shown in panels A and B and the curves for the single-substrate solutions are shown in Appendix D (Supporting Information).

https://dx.doi.org/10.1021/acs.jafc.0c05924
J. Agric. Food Chem. 2021, 69, 2295−2305

concentrations (Figure 2A). By 2 h, about 85% of the peaked ADP concentration (355 ± 9 μM) was dephosphorylated, accompanied by a peaked AMP concentration of 170 ± 4 μM (Figure 2A). A gradual dephosphorylation of AMP subsequently occurred in the subsequent 22 h (Figure 2A). In contrast to the relatively rapid dephosphorylation of the multiphosphorylated substrates in the initial hours of reaction time, only 14% of monophosphorylated sugars (i.e., R5P and G6P) was dephosphorylated after 6 h, indicating limited PhyA reactivity toward the latter substrates (Figure 2A). After 48 h, the concentrations of the sugar by-products (i.e., glucose from G6P, ribose from R5P, and fructose from FBP) reached 238, 155, and 648 μM, respectively (Supporting Information Appendix E). We found that the higher level of ribose concentration, relative to what would be expected solely from R5P dephosphorylation, was due to the degradation of adenosine (composed of a ribose attached to an adenine base) by the PhyA extract (Supporting Information Appendix D).

To determine the influence of the endogenous substrate on the PhyA reactivity, we conducted a separate experiment with the same mixture of P_o compounds in the absence of myo-IP_6 (Figure 2B). In this scenario, dephosphorylation of both FBP and ATP was complete after only 30 s, compared to 20 min in the presence of myo-IP_6 (Figure 2A,B). The corresponding dephosphorylated products, F6P and ADP, also reached their highest concentrations (respectively, 302 ± 18 and 441 ± 38 μM) by the 30 s reaction time (Figure 2B). Moreover, by the first 6 h, 50% of G6P and 33% of R5P remained in solution in the absence of myo-IP_6, compared to more than 80% in the presence of myo-IP_6 (Figure 2A,B). A faster increase of the final sugar and nucleoside by-products (i.e., glucose, fructose, ribose, and adenosine) was also observed in the absence of myo-IP_6 (Figure 2B). Therefore, our data highlight the capability of PhyA to catalyze the dephosphorylation of other P_o compounds commonly found in soils in a hierarchical manner, both in the presence and absence of myo-IP_6. To investigate quantitatively the hierarchy of PhyA-mediated P_o hydrolysis, we determine the transformation rates based on the kinetic decay of P_o concentrations (Figure 2C).

Substrate Dephosphorylation Rates in Mixed-Substrate versus Single-Substrate Solutions. Using eqs 1−6 and the nonlinear regression of the kinetic data, we obtained the dephosphorylation rate coefficients for each P_o substrate across three experimental conditions: single-substrate solutions, mixed-substrate solution with myo-IP_6, and mixed-substrate solution without myo-IP_6 (Figure 2C; Supporting Information Appendix D). In the single-substrate reactions, the hierarchy of substrate dephosphorylation was as follows: ATP = FBP > ADP > AMP = R5P > G6P > F6P (Figure 2C, Supporting Information Appendix F). In the mixed-substrate experiments containing or lacking myo-IP_6, there was a similar hierarchy, except that there was no preference between R5P and G6P (Figure 2C, Supporting Information Appendix F). Compared to both the single-substrate experiment and the mixed-substrate experiment without myo-IP_6, there was a 34-fold decrease in the rate coefficients of ATP and FBP with the mixed-substrate experiment with myo-IP_6, thus highlighting myo-IP_6 as a direct competitor to these two multiphosphorylated compounds for PhyA reactivity (Figure 2C, Supporting Information Appendix F). Interestingly, in both mixed-substrate experiments, the ADP dephosphorylation rate was 8 times less than that in the single-substrate experiment, implying inhibition of ADP dephosphorylation by ATP and FBP (Figure 2C, Supporting Information Appendix F). Regarding the low rate coefficient determined for the single-substrate dephosphorylation of the monophosphorylated compounds, this remained the same for G6P for both mixed-substrate scenarios, but this value for AMP, R5P, and F6P decreased by up to 2.5, 4 and 6 times, respectively, for one or both mixed-substrate experiments (Figure 2C, Supporting Information Appendix F). Detailed in the next section are the contributions of the substrate-specific P_i recycling from the different P_o compounds in the mixture.

Hierarchical P_i Recycling from a Mixture of P_o Substrates. Using the simultaneous monitoring of P_o substrates and their by-products, we were able to profile the substrate-specific P_i contribution relative to their total P_i-equivalent potentials catalyzed by the PhyA extract that reacted with the mixture of P_o compounds (Figure 3). In the mixture containing myo-IP_6, all the P_i that could be derived from myo-IP_6 was recycled in less than 5 min (Figure 3A). After myo-IP_6, the multiphosphorylated P_o substrates (i.e., ATP, FBP, and ADP) had the fastest and highest contributions of recycled P_i (Figure 3A). With myo-IP_6 present in the mixture, it took 1 h

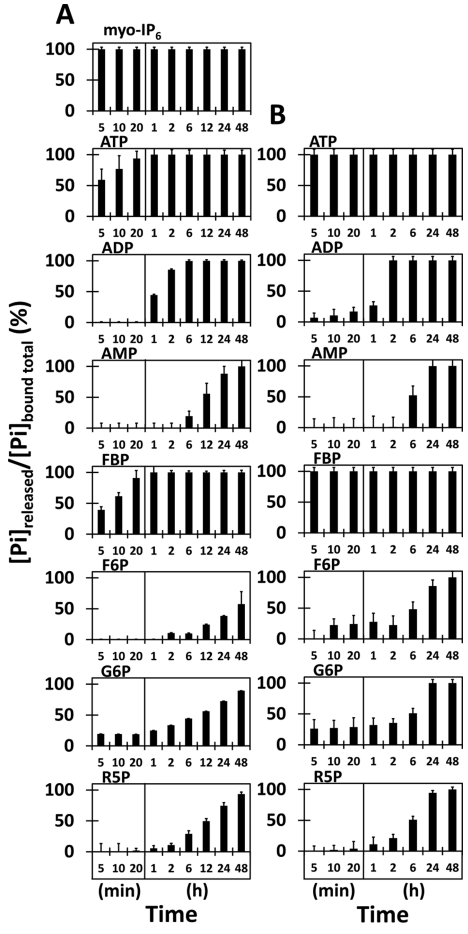

Figure 3. Percentage contributions of different P_o compounds in phytase-catalyzed P_i-recycling in a mixture containing myo-IP_6 (A) and a mixture without myo-IP_6 (B) during the time. The first three time points are presented as min and the rest of the time points are in h unit. The contribution of a specific P_o compound in P_i recycling is shown as the percentage of its associated released P_i ($[P_i]_{released}$) over its total P_i-equivalent potentials ($[P_i]_{bound\ total}$).

https://dx.doi.org/10.1021/acs.jafc.0c05924
J. Agric. Food Chem. 2021, 69, 2295−2305

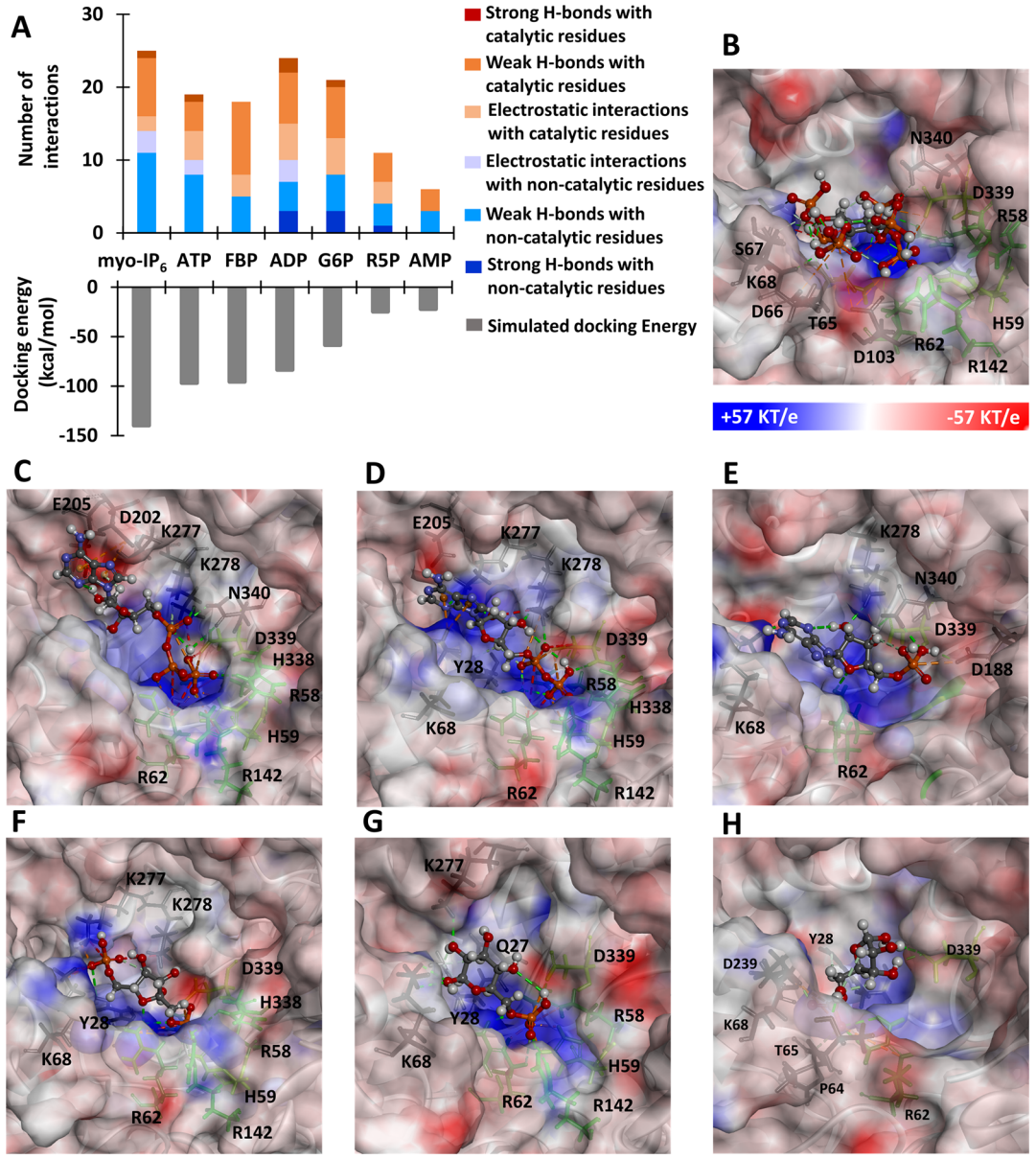

Figure 4. Interactions, docking energies, and structures of simulated compound-PhyA complexes. (A, top) Distribution of different types of interactions: strong H-bonds with catalytic residues (dark red), weak H-bonds with catalytic residues (dark orange), electrostatic interactions with catalytic residues (light orange), electrostatic interactions with non-catalytic residues (light purple), weak H-bonds with non-catalytic residues (light blue), strong H-bonds with non-catalytic residues (dark blue). (A, bottom). Calculated docking energy for the optimized configuration of each compound-PhyA complex. Docked structures of each P_o compound within the active site of PhyA: myo-IP_6 (B), ATP (C), ADP (D), AMP (E), FBP (F), G6P (G), R5P (H). Hydrogen bonding and electrostatic interactions are shown in green and orange dashed lines, respectively; electrostatic surface map of the active site indicates positively-charged (blue), negatively-charged (red), and neutral (white) regions. The criterion parameters for determining the different type of interactions and the docking energies are detailed in the Materials and Methods section.

to achieve the complete recycling of P_i from ATP and FBP, and only 20% G6P-derived P_i was in solution (Figure 3A). However, in the absence of myo-IP_6, P_i recycling from ATP and FBP was completed within 5 min, as well as up to 40% of G6P-derived P_i (Figure 3B). For the two ATP by-products, it took greater than 20 min to obtain P_i recycled from ADP in the presence of myo-IP_6, but 10% of the ADP-derived P_i was already recycled by 10 min in the absence of myo-IP_6; by 6 h, only 20% and over 50% of AMP-P_i were recycled in the presence and absence of myo-IP_6, respectively (Figure 3). At 2 h reaction time, in the presence of myo-IP_6, only about 10% of the P_i from R5P and F6P was recycled, but about 33−35% of the total P_i from G6P were recycled (Figure 3). Subsequently, the hydrolysis of ADP (from dephosphorylated ATP) was initiated, with 100% of the ADP-derived-P_i recycled within 6 h (Figure 3A). At the end of the reaction time (48 h), 57, 89, and 93% of the total P_i from, respectively, F6P, G6P, and R5P were recycled in the presence of myo-IP_6; complete P_i recycling from these compounds was achieved in the absence of myo-IP_6 (Figure 3).

In summary, the presence of myo-IP_6 was found to impede P_i recycling from multiphosphorylated substrates and, to a lesser extent, from monophosphorylated substrates (Figure 3A). Following dephosphorylation of myo-IP_6, PhyA was able to catalyze the recycling of 100% of the potential equivalent P_i from multiphosphorylated compounds (ATP, ADP, and FBP);

https://dx.doi.org/10.1021/acs.jafc.0c05924
J. Agric. Food Chem. 2021, 69, 2295−2305

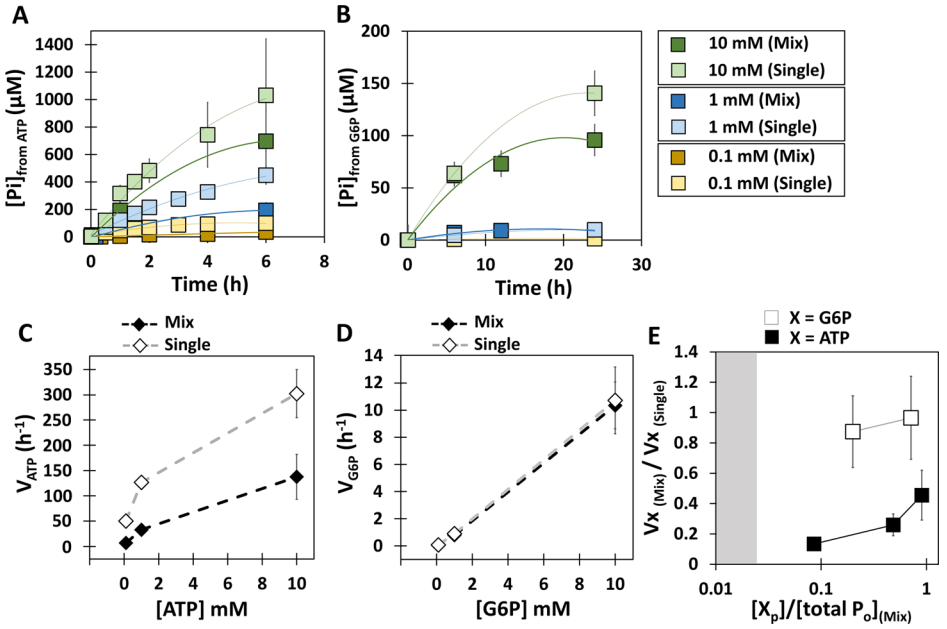

Figure 5. Progress curves of P_i recycling from ATP (A) and G6P (B), in the presence of a mixture of competing substrates (mix) or in single substrate solution (single), at three initial concentrations: 0.1, 1 and 10 mM. In B and D, no values are reported for the reaction of 0.1 mM G6P in the mixture because P_i concentration was below the limit of detection. The initial rates of dephosphorylation (V) are plotted against the concentration of the substrates, ATP (C) and G6P (D), in the mixed-substrate (mix) and the single-substrate (single) reactions. (E) The effect of mixture on the rate of dephosphorylation is shown by plotting the ratio $V_{X(mix)}$ over $V_{X(single)}$ against the fractional amount of total P in the mixture of P_o compounds was found in the target substrates (X = G6P or ATP). The gray area represents the fractional P (less than 0.025) content whereby V values could not be determined for the mixed-substrate reactions. Datasets and statistical analyses are listed in Appendix G and Appendix H (Supporting Information).

this recycling was initiated earlier and completed by 48 h in the absence of myo-IP_6 (Figure 3A,B). Interestingly, even after 48 h, a fraction of parent monophosphorylated compounds still remained, which we attributed to the apparent low dephosphorylation rate coefficient of these compounds (Figure 2C). To explore the structural basis for the experimentally determined hierarchy of PhyA reactivity, we conducted molecular docking simulations to probe the binding mechanisms of each P_o substrate within the PhyA active site.

Docking Energies, Theoretical Interactions, and Mechanisms of Substrate Selectivity of PhyA. We simulated the docking of the following seven P_o compounds within the active site of PhyA: myo-IP_6, ATP, FBP, ADP, AMP, G6P, and R5P (Figure 4A–H). Expectedly, the endogenous substrate of PhyA (myo-IP_6) had the most thermodynamically favorable docking energy (i.e., lowest docking energy) and the highest number of interactions with the active site (including strong and weak H-bonding and electrostatic interactions) (Figure 4A). The PhyA active site, which consists of six conserved residues (R58, H59, R62, R142, H338, and D339) required for the catalytic process,[29] is characterized by positive electrostatic potentials that favor the binding of the highly negatively charged myo-IP_6[15] (Figure 4B). The catalytic nucleophile and proton donor residues (i.e., H59 and D339)[29] were involved in H-bonding and electrostatic interactions with phosphate groups of myo-IP_6 (Figure 4B). Moreover, the conserved positively charged residues, R62 and R142, mediated H-bonds with the P3-associated O atoms of myo-IP_6 (Figure 4B). Along with these catalytically important interactions, other interactions between the phosphate groups and nonconserved residues close to the active site provided a favorable and stable orientation of myo-IP_6 for catalysis (Figure 4B).

Both ATP and FBP exhibited about the same total number of interactions with the substrate binding pocket as well as similar docking energies (Figure 4A), consistent with the similar preference of PhyA for these substrates deduced from the experimental data (Figures 2C and 3). Also, in agreement with the kinetic rate coefficients, ADP had a less favorable docking energy than both ATP and FBP (Figures 2C and 4A). The three phosphate groups of ATP mediated interactions with the active site residues (Figure 4C). Specifically, the ATP terminal phosphate (P3) was involved in direct or O-mediated H-bonds with the catalytic residues (H59 and D339), while facilitating H-bonding and electrostatic interactions with other conserved residues in the active site (H338, R58, and R62) (Figure 4C). The adenosine moiety of ATP interacted with an electronegative region through three π-anions with two negatively charged residues (Figure 4C). In a similar manner to ATP, ADP was stretched out along the pocket with the terminal phosphate group surrounded by interactions from the active site cavity (Figure 4D). The adenosine moiety of ADP was stabilized by strong H-bond and π-bond interactions through the ribose and adenine moieties, respectively (Figure 4D). This stabilization of the ADP adenosine moiety would reduce the substrate flexibility in the active site, which may be responsible for the less favorable transformation kinetics of ADP relative to those of ATP and FBP (Figure 2C).

With respect to the FBP binding, the positive electrostatic surface of PhyA was narrowly localized around the phosphate groups (Figure 4F). One of the phosphate moieties of FBP interacted strongly with the entire set of conserved active site residues (R58, H59, D339, H338, R62, and R142) and the other phosphate was stabilized further away interacting with a electropositive region in the binding pocket (Figure 4F). We found that FBP exhibited more substrate flexibility in the active

https://dx.doi.org/10.1021/acs.jafc.0c05924
J. Agric. Food Chem. 2021, 69, 2295−2305

site than ADP because of the smaller size of fructose moiety relative to that of adenosine moiety in ADP, which may explain the faster dephosphorylation kinetics of FBP compared to that of ADP (Figures 2C and 4F).

In agreement with the experimental kinetic data, the least favorable docking energies were found for the monophosphorylated substrates (i.e. G6P, R5P, and AMP) and the lowest number of interactions were found for AMP and R5P (Figures 2C and 4A). While the phosphate group of either AMP and R5P was not involved in any interaction with the catalytic residues, the ribose moieties in these compounds mediated interactions with the active site (Figure 4E,H). Compared to AMP and R5P, a relatively more desirable interaction network was observed for G6P in the active site (Figure 4E,G,H). However, while the O atoms associated with the phosphate group of G6P formed H-bonds with five conserved residues in the active site, the glucose moiety was also stabilized via H-bonds with four noncatalytic positive residues (Figure 4G), leading to reduced structural flexibility of G6P in the active site. Considering the experimentally and theoretically determined preference of PhyA for multiphosphorylated P_o compounds over monophosphorylated ones, we chose two representatives from these P_o substrates (ATP and G6P) to investigate the mixture effects on the initial dephosphorylation rates of each substrate as a function of different concentrations in the mixture.

Concentration-Dependent Effect of Internal Competition in Mixed-Substrate Reactions. Separate experiments were performed at three initial concentrations of ATP and G6P (0.1, 1, and 10 mM) in the presence or absence of a mixture of competing substrates (Figure 5A,B). We obtained the initial rates of P_i recycling from the time-dependent substrate hydrolysis in the mixed-substrate and single-substrate conditions (Figure 5C,D, Supporting Information Appendix G). In accordance with the aforementioned hierarchy in substrate preference, we found that the single-substrate hydrolysis rates at initial substrate concentrations of 1 and 10 mM for ATP were 141-fold and 28-fold higher than the corresponding hydrolysis rates for G6P (Figure 5C,D).

With respect to the substrate hydrolysis in the mixed-substrate conditions, we observed different behaviors of PhyA activity toward each substrate (Figure 5D,E). On the one hand, a linear increase in the rates of G6P hydrolysis was again observed by increasing the G6P concentration but the rates obtained with the mixture remained the same as the ones obtained with the single-substrate scenario despite a 10-fold increase in the G6P concentration (from 1 to 10 mM) in the mixture (Figure 5D,E); there was no hydrolysis of G6P at the 0.1 mM G6P experiments in the mixture (Figure 5B,D). On the other hand, the rates of ATP hydrolysis increased as the fractional amount of ATP in the mixture increased, but these values were lower than the rates in the single-substrate conditions (Figure 5D). Moreover, we found that the inhibitory effect of the presence of competitive substrates was reduced as the ATP concentration increased in the mixture (Figure 5E, Supporting Information Appendix G). Specifically, comparing the mixed-substrate data to the single-substrate data, there was a 7-fold decrease in the hydrolysis rate for 0.1 mM ATP, whereas there was only a 2-fold decrease in the hydrolysis rate for 10 mM ATP (Figure 5E, Supporting Information Appendix G). However, the decreasing slope in the profile of the increased rate of ATP hydrolysis highlighted that the maximum rate for ATP hydrolysis would be lower with the mixture than in the single-substrate conditions, indicating that increasing ATP concentration would not fully remove the internal competition by the other substrates in the mixture (Figure 5C).

DISCUSSION

Phosphatase-type enzymes including phytases can play an important role in P recycling from P_o compounds in agricultural soils.[8,9] In relevance to increasing plant-available P, the soil around the plant rhizosphere is enriched in organic matter containing a mixture of P_o compounds.[3,41] Therefore, understanding the reactivity of phosphatases in a mixture of P_o compounds is of particular interest. Previous studies on the activity of PhyA, which were conducted only with single-substrate solutions,[18−20] have indicated myo-IP_6 as the preferred substrate for PhyA[18−20] which is in agreement with the substrate preference observed in our study but inconsistent with a higher activity of PhyA for G6P than for myo-IP_6 reported by George et al.[20] Regarding the hierarchical substrate preference of PhyA across different P_o compounds based on single-substrate reactions, Greiner et al.[21] reported the highest activity rate with myo-IP_6, followed by, in a decreasing order, ADP, AMP, ATP, and G6P; by contrast, Casey and Walsh[19] reported higher activity for AMP than for ADP; and Sariyska et al.[18] reported G6P as the preferred substrate, followed by ATP, AMP, and ADP. Therefore, based on the reported discrepant findings from single-substrate experiments, it is challenging to determine substrate selectivity in environmentally relevant mixed-substrate reactions.

Our application of high-resolution LC−MS offers an approach for probing the P_i-recycling activity of PhyA reacted with a mixture of P_o substrates. Such LC−MS-based analysis would be instrumental in conducting subsequent comprehensive enzyme kinetic studies of PhyA and other phosphatases. Within the scope of this study, our findings provide mechanistic insights into the hierarchical reactivity of PhyA toward a mixture of diverse P_o compounds consisting of myo-IP_6, sugar phosphates, ribonucleotides, and metabolic intermediates. Our experimental data captured the dephosphorylation activity toward all investigated compounds, but the reactions kinetics were faster for the multiphosphorylated compounds than for the monophosphorylated ones. Our molecular docking simulations revealed that the positively charged potential surface along the enzyme's active site facilitated favorable binding interactions with multiphosphorylated compounds, which were consistent with the substrate hierarchy observed experimentally. Consistent with the slow dephosphorylation kinetics measured for the monophosphorylated compounds, the simulation results revealed that these compounds adopted unfavorable binding orientations within the substrate-binding pocket. In addition to these electrostatic attractions revealed by the molecular docking data, we posit that steric hindrance may influence the substrate−enzyme interactions. For instance, in accordance with the findings of a recent study on purple acid phosphatases,[42] the spacious active site of PhyA might better accommodate the binding of the large substrates than the smaller ones.

It is well established that a competitive inhibition can occur when two substrates are reacted with the same enzyme.[43] Here, we found that the presence of a mixture containing several competitive substrates decreases the dephosphorylation rates of a favorable substrate (ATP) compared to the single-substrate scenarios, but this mixture-induced inhibition was

https://dx.doi.org/10.1021/acs.jafc.0c05924
J. Agric. Food Chem. 2021, 69, 2295−2305

not exhibited for a nonfavorable substrate (G6P). The inhibitory effect of the mixture on ATP hydrolysis was relieved by increasing the substrate concentration in the mixture. The lack of inhibitory effect of the mixture on the rates of P_i recycling from G6P could be due to persistent low activity for the nonfavorable substrates (i.e., monophosphorylated compounds) in the presence of other substrates. Nevertheless, such low-affinity phosphatase reactions on organic mixtures within agricultural soils could contribute sugars and nucleosides as byproducts, which can be incorporated subsequently into soil microbial carbon metabolism.

Given the wide distribution of phytases and other phosphatases secreted by plants, bacteria, and fungi,[8,9] our data thus highlight the potential role of these enzymes to contribute to the cycling of both phosphorus and carbon in agricultural soils.[44] Acknowledging the potential adsorption of both P_o compounds[4,6,45] and phosphatase enzymes[6,46−48] on soil minerals, an important next step is to investigate the influence of minerals on the substrate hierarchy for the enzyme reactivity determined here. It was reported previously[46] that adsorption of an alkaline phosphatase on a clay (montmorillonite) and iron-oxyhydroxide mineral (goethite) led to reduction in enzymatic reactivity toward a synthetic P_o compound (*para*-nitrophenyl phosphate). However, relative to enzyme activity in solution, another study[7] reported that adsorption to goethite did not change the activity of an acid phosphatase reacted with a sugar phosphate. Olsson et al.[6] proposed that minerals could preserve acid phosphatase reactions by concentrating the co-presence of enzyme and substrate on the mineral surface. Furthermore, Leprince and Quiquampoix[48] posited that clay minerals can enhance the stability of acid phosphatase enzymes. These previous findings imply that the hierarchical reactivity determined here for PhyA, an acid phosphatase, may be maintained in the presence of soil minerals. Subsequent investigations are needed to evaluate the effects of soil minerals on the activity of phosphatase enzymes in the presence of a mixture of P_o compounds. Furthermore, toward improving our forecasting of enzyme-mediated P_i recycling from soil organic matter, further mechanistic insights are warranted regarding the reactivity of phosphatase-type enzymes of different biological origins (i.e., from plant, fungi, and bacteria) present in agricultural soils.

■ ASSOCIATED CONTENT

Supporting Information

The Supporting Information is available free of charge at https://pubs.acs.org/doi/10.1021/acs.jafc.0c05924.

Details of materials, chromatographic procedure and inorganic P analysis, governing equations of kinetic models of enzymatic hydrolysis, single-substrate experimental data and kinetic modeling, mixed-substrate experimental data and kinetic modeling, transformation coefficients of P_o compounds, initial rates of dephosphorylation at different concentrations of ATP and G6P, statistical analysis of initial rate differences in mixture and single-substrate reactions for ATP and G6P, standard deviation calculation for the ratios of initial rates based on the Taylor series method, and interaction criteria for molecular modeling simulations (PDF)

■ AUTHOR INFORMATION

Corresponding Author

Ludmilla Aristilde − *Department of Biological and Environmental Engineering, College of Agriculture and Life Sciences, Cornell University, Ithaca, New York 14853, United States; Department of Civil and Environmental Engineering, McCormick School of Engineering and Applied Science, Northwestern University, Evanston, Illinois 60208, United States;* orcid.org/0000-0002-8566-1486; Phone: 847-491-2999; Email: ludmilla.aristilde@northwestern.edu

Authors

Mina Solhtalab − *Department of Biological and Environmental Engineering, College of Agriculture and Life Sciences, Cornell University, Ithaca, New York 14853, United States*

Annaleise R. Klein − *Department of Biological and Environmental Engineering, College of Agriculture and Life Sciences, Cornell University, Ithaca, New York 14853, United States; Department of Civil and Environmental Engineering, McCormick School of Engineering and Applied Science, Northwestern University, Evanston, Illinois 60208, United States*

Complete contact information is available at: https://pubs.acs.org/10.1021/acs.jafc.0c05924

Notes

The authors declare no competing financial interest.

■ ACKNOWLEDGMENTS

This research was supported by a grant from the National Science Foundation (award # 1709626).

■ REFERENCES

(1) Zhao, Z.; Wang, S.; White, P. J.; Wang, Y.; Shi, L.; Xu, F. Boron and Phosphorus Act Synergistically to Modulate Absorption and Distribution of Phosphorus and Growth of Brassica Napus. *J. Agric. Food Chem.* **2020**, *68*, 7830−7838.

(2) Meyer, G.; Bell, M. J.; Doolette, C. L.; Brunetti, G.; Zhang, Y.; Lombi, E.; Kopittke, P. M. Plant-Available Phosphorus in Highly Concentrated Fertilizer Bands: Effects of Soil Type, Phosphorus Form, and Coapplied Potassium. *J. Agric. Food Chem.* **2020**, *68*, 7571−7580.

(3) Zhang, Y.; Wang, X.; Xu, F.; Song, T.; Du, H.; Gui, Y.; Xu, M.; Cao, Y.; Dang, X.; Rensing, C.; et al. Combining Irrigation Scheme and Phosphorous Application Levels for Grain Yield and Their Impacts on Rhizosphere Microbial Communities of Two Rice Varieties in a Field Trial. *J. Agric. Food Chem.* **2019**, *67*, 10577−10586.

(4) Wang, X.; Hu, Y.; Tang, Y.; Yang, P.; Feng, X.; Xu, W.; Zhu, M. Phosphate and Phytate Adsorption and Precipitation on Ferrihydrite Surfaces. *Environ. Sci.: Nano* **2017**, *4*, 2193−2204.

(5) Turner, B. L.; Newman, S.; Newman, J. M. Organic Phosphorus Sequestration in Subtropical Treatment Wetlands. *Environ. Sci. Technol.* **2006**, *40*, 727−733.

(6) Olsson, R.; Giesler, R.; Loring, J. S.; Persson, P. Enzymatic Hydrolysis of Organic Phosphates Adsorbed on Mineral Surfaces. *Environ. Sci. Technol.* **2012**, *46*, 285−291.

(7) McLaren, T. I.; Smernik, R. J.; McLaughlin, M. J.; McBeath, T. M.; Kirby, J. K.; Simpson, R. J.; Guppy, C. N.; Doolette, A. L.; Richardson, A. E. Complex Forms of Soil Organic Phosphorus-A Major Component of Soil Phosphorus. *Environ. Sci. Technol.* **2015**, *49*, 13238−13245.

(8) Cabugao, K. G.; Timm, C. M.; Carrell, A. A.; Childs, J.; Lu, T.-Y. S.; Pelletier, D. A.; Weston, D. J.; Norby, R. J. Root and Rhizosphere

Bacterial Phosphatase Activity Varies with Tree Species and Soil Phosphorus Availability in Puerto Rico Tropical Forest. *Front. Plant Sci.* **2017**, *8*, 1−14.
(9) Margalef, O.; Sardans, J.; Fernández-Martínez, M.; Molowny-Horas, R.; Janssens, I. A.; Ciais, P.; Goll, D.; Richter, A.; Obersteiner, M.; Asensio, D.; et al. Global Patterns of Phosphatase Activity in Natural Soils. *Sci. Rep.* **2017**, *7*, 1−13.
(10) Singh, B.; Satyanarayana, T. Microbial Phytases in Phosphorus Acquisition and Plant Growth Promotion. *Physiol. Mol. Biol. Plants* **2011**, *17*, 93−103.
(11) Yao, Q.; Li, Z.; Song, Y.; Wright, S. J.; Guo, X.; Tringe, S. G.; Tfaily, M. M.; Paša-Tolić, L.; Hazen, T. C.; Turner, B. L.; et al. Community Proteogenomics Reveals the Systemic Impact of Phosphorus Availability on Microbial Functions in Tropical Soil. *Nat. Ecol. Evol.* **2018**, *2*, 499−509.
(12) Greiner, R. Activity of Escherichia Coli, Aspergillus Niger, and Rye Phytase toward Partially Phosphorylated Myo-Inositol Phosphates. *J. Agric. Food Chem.* **2017**, *65*, 9603−9607.
(13) Ahn, D. J.; Won, J. G.; Rico, C. M.; Lee, S. C. Influence of Variety, Location, Growing Year, and Storage on the Total Phosphorus, Phytate-Phosphorus, and Phytate-Phosphorus to Total Phosphorus Ratio in Rice. *J. Agric. Food Chem.* **2010**, *58*, 3008−3011.
(14) Romano, N.; Kumar, V. Phytase in Animal Feed. In *Enzymes in Human and Animal Nutrition: Principles and Perspectives*; Elsevier Inc., 2018; Vol. *73*−*88*
(15) Oh, B.-C.; Choi, W.-C.; Park, S.; Kim, Y.-o.; Oh, T.-K. Biochemical Properties and Substrate Specificities of Alkaline and Histidine Acid Phytases. *Appl. Microbiol. Biotechnol.* **2004**, *63*, 362−372.
(16) van Hartingsveldt, W.; van Zeijl, C. M. J.; Harteveld, G. M.; Gouka, R. J.; Suykerbuyk, M. E. G.; Luiten, R. G. M.; van Paridon, P. A.; Selten, G. C. M.; Veenstra, A. E.; van Gorcom, R. F. M.; et al. Cloning, Characterization and Overexpression of the Phytase-Encoding Gene (PhyA) of Aspergillus Niger. *Gene* **1993**, *127*, 87−94.
(17) Tan, Y.; Cui, Y.; Li, H.; Kuang, A.; Li, X.; Wei, Y.; Ji, X. Rhizospheric Soil and Root Endogenous Fungal Diversity and Composition in Response to Continuous Panax Notoginseng Cropping Practices. *Microbiol. Res.* **2017**, *194*, 10−19.
(18) Sariyska, M. V.; Gargova, S. A.; Koleva, L. A.; Angelov, A. I. Aspergillus Niger Phytase: Purification and Characterization. *Biotechnol. Biotechnol. Equip.* **2005**, *19*, 98−105.
(19) Casey, A.; Walsh, G. Purification and Characterization of Extracellular Phytase from Aspergillus Niger ATCC 9142. *Bioresour. Technol.* **2003**, *86*, 183−188.
(20) George, T. S.; Simpson, R. J.; Gregory, P. J.; Richardson, A. E. Differential Interaction of Aspergillus Niger and Peniophora Lycii Phytases with Soil Particles Affects the Hydrolysis of Inositol Phosphates. *Soil Biol. Biochem.* **2007**, *39*, 793−803.
(21) Greiner, R.; Silva, L. G. d.; Couri, S. Purification and Characterisation of an Extracellular Phytase from *Aspergillus niger* 11T53A9. *Braz. J. Microbiol.* **2009**, *40*, 795−807.
(22) Cornish-Bowden, A. *Fundamentals of Enzyme Kinetics*, 4th ed.; Wiley-Black Well: Marseille, France, 2013.
(23) Schellenberger, V.; Siegel, R. A.; Rutter, W. J. Analysis of Enzyme Specificity by Multiple Substrate Kinetics. *Biochemistry* **1993**, *32*, 4344−4348.
(24) Kuo, Y.-M.; Henry, R. A.; Andrews, A. J. Measuring Specificity in Multi-Substrate/Product Systems as a Tool to Investigate Selectivity in Vivo. *Biochim. Biophys. Acta Protein Proteonomics* **2016**, *1864*, 70−76.
(25) Deng, Z.; Mao, J.; Wang, Y.; Zou, H.; Ye, M. Enzyme Kinetics for Complex System Enables Accurate Determination of Specificity Constants of Numerous Substrates in a Mixture by Proteomics Platform. *Mol. Cell. Proteomics* **2017**, *16*, 135−145.
(26) Kellerman, D. L.; Simmons, K. S.; Pedraza, M.; Piccirilli, J. A.; York, D. M.; Harris, M. E. Determination of Hepatitis Delta Virus Ribozyme N(-1) Nucleobase and Functional Group Specificity Using Internal Competition Kinetics. *Anal. Biochem.* **2015**, *483*, 12−20.
(27) Anderson, V. E. Multiple Alternative Substrate Kinetics. *Biochim. Biophys. Acta Protein Proteonomics* **2015**, *1854*, 1729−1736.
(28) Clesceri, L.; Greensberg, A.; Eaton, A. *Standard Methods for the Examination of Water and Wastewater*, 51st ed.; Clesceri, L., Greensberg, A., Eaton, A., Eds.; Am. J. Public Health: Washington DC, 1999.
(29) Oakley, A. J. The Structure of Aspergillus Niger Phytase PhyA in Complex with a Phytate Mimetic. *Biochem. Biophys. Res.* **2010**, *397*, 745−749.
(30) Liu, Q.; Huang, Q.; Lei, X. G.; Hao, Q. Crystallographic Snapshots of Aspergillus Fumigatus Phytase, Revealing Its Enzymatic Dynamics. *Structure* **2004**, *12*, 1575−1583.
(31) Mulholland, A. J. Modelling Enzyme Reaction Mechanisms, Specificity and Catalysis. *Drug Discov. Today* **2005**, *10*, 1393−1402.
(32) Aristilde, L.; Reed, M. L.; Wilkes, R. A.; Youngster, T.; Kukurugya, M. A.; Katz, V.; Sasaki, C. R. S. Glyphosate-Induced Specific and Widespread Perturbations in the Metabolome of Soil Pseudomonas Species. *Front. Environ. Sci.* **2017**, *5*, 1−13.
(33) Barzen-Hanson, K. A.; Wilkes, R. A.; Aristilde, L. Quantitation of Carbohydrate Monomers and Dimers by Liquid Chromatography Coupled with High-Resolution Mass Spectrometry. *Carbohydr. Res.* **2018**, *468*, 30−35.
(34) Kendall, M. G.; Stuart, A. *Kendall's Advanced Theory of Statistics*, 6th ed.; Wiley: London, 1998.
(35) Accelry's. *Discovery Studio Modeling Environment*; Accelrys Software Inc.: San Diego, 2013.
(36) Flannelly, D. F.; Aoki, T. G.; Aristilde, L. Short-Time Dynamics of PH-Dependent Conformation and Substrate Binding in the Active Site of Beta-Glucosidases: A Computational Study. *J. Struct. Biol.* **2015**, *191*, 352−364.
(37) Solhtalab, M.; Flannelly, D. F.; Aristilde, L. Substrate Binding versus Escape Dynamics in a PH-Affected Fungal Beta-Glucosidase Revealed by Molecular Dynamics Simulations. *Carbohydr. Res.* **2019**, *472*, 127.
(38) Jiang, S.; Zhang, L.; Cui, D.; Yao, Z.; Gao, B.; Lin, J.; Wei, D. The Important Role of Halogen Bond in Substrate Selectivity of Enzymatic Catalysis. *Sci. Rep.* **2016**, *6*, 34750.
(39) Wu, G.; Robertson, D. H.; Brooks, C. L.; Vieth, M. Detailed Analysis of Grid-Based Molecular Docking: A Case Study of CDOCKER—A CHARMm-Based MD Docking Algorithm. *J. Comput. Chem.* **2003**, *24*, 1549−1562.
(40) Desiraju, G. R. A Bond by Any Other Name. *Angew. Chem. Int. Ed.* **2011**, *50*, 52−59.
(41) McDowell, R. W.; Stewart, I. The Phosphorus Composition of Contrasting Soils in Pastoral, Native and Forest Management in Otago, New Zealand: Sequential Extraction and 31P NMR. *Geoderma* **2006**, *130*, 176−189.
(42) Feder, D.; McGeary, R. P.; Mitić, N.; Lonhienne, T.; Furtado, A.; Schulz, B. L.; Henry, R. J.; Schmidt, S.; Guddat, L. W.; Schenk, G. Structural Elements That Modulate the Substrate Specificity of Plant Purple Acid Phosphatases: Avenues for Improved Phosphorus Acquisition in Crops. *Plant Sci.* **2020**, *294*, 110445.
(43) Hammershøj, R.; Birch, H.; Redman, A. D.; Mayer, P. Mixture Effects on Biodegradation Kinetics of Hydrocarbons in Surface Water: Increasing Concentrations Inhibited Degradation Whereas Multiple Substrates Did Not. *Environ. Sci. Technol.* **2019**, *53*, 3087−3094.
(44) Reed, S. C.; Yang, X.; Thornton, P. E. Incorporating Phosphorus Cycling into Global Modeling Efforts: A Worthwhile, Tractable Endeavor. *New Phytol.* **2015**, *208*, 324−329.
(45) Klein, A. R.; Bone, S. E.; Bakker, E.; Chang, Z.; Aristilde, L. Abiotic Phosphorus Recycling from Adsorbed Ribonucleotides on a Ferrihydrite-Type Mineral: Probing Solution and Surface Species. *J. Colloid Interface Sci.* **2019**, *547*, 171−182.
(46) Zhu, Y.; Wu, F.; Feng, W.; Liu, S.; Giesy, J. P. Interaction of Alkaline Phosphatase with Minerals and Sediments: Activities, Kinetics and Hydrolysis of Organic Phosphorus. *Colloids Surf., A* **2016**, *495*, 46−53.
(47) Giaveno, C.; Celi, L.; Richardson, A. E.; Simpson, R. J.; Barberis, E. Interaction of Phytases with Minerals and Availability of

https://dx.doi.org/10.1021/acs.jafc.0c05924
J. Agric. Food Chem. 2021, 69, 2295−2305

Substrate Affect the Hydrolysis of Inositol Phosphates. *Soil Biol. Biochem.* **2010**, *42*, 491−498.
(48) Leprince, F.; Quiquampoix, H. Activité Enzymatique Extracellulaire Dans Ie Sol: Effet Du PH et de La Force Ionique Sur l'interaction Avec La Montmorillonite de Deux Phosphates Acides Sécrdteés Par Le Champignon Ectomycorhizien Hebeloma Cylindrosporum. *Eur. J. Soil Sci.* **1996**, *47*, 511−522.
(49) Sun, M.; Alikhani, J.; Massoudieh, A.; Greiner, R.; Jaisi, D. P. Phytate Degradation by Different Phosphohydrolase Enzymes: Contrasting Kinetics, Decay Rates, Pathways, and Isotope Effects. *Soil Sci. Soc. Am. J.* **2017**, *81*, 61−75.
(50) Zeller, E.; Schollenberger, M.; Kühn, I.; Rodehutscord, M. Hydrolysis of Phytate and Formation of Inositol Phosphate Isomers without or with Supplemented Phytases in Different Segments of the Digestive Tract of Broilers. *J. Nutr. Sci.* **2015**, *4*, 1−12.

https://dx.doi.org/10.1021/acs.jafc.0c05924
J. Agric. Food Chem. 2021, 69, 2295−2305